International Journal of Mass Spectrometry 178 (1998) 129–141

Eliminating the interference of M-nH ions in isotope patterns from low-resolution mass spectra

Maria C.B. Moraes, José G.A. Brito Neto, Valmir F. Juliano[1], Claudimir L. do Lago*

Departamento de Química Fundamental, Instituto de Química, Universidade de São Paulo, Av. Prof. Lineu Prestes 748, CEP 05508-900, São Paulo-SP, Brazil

Received 23 March 1998; accepted 28 June 1998

Abstract

The occurrence of ions that differ by one or more hydrogen atoms (M-nH) is very common in mass spectrometry. In this article, we introduce a chemometric method (M-nH method) that allows one to eliminate this interference over the isotope pattern of the M ion. A reasonably simple mathematical formulation is achieved by disregarding the deuterium abundance for the hydrogen atoms involved in the fragmentation process. The resulting nonlinear system of equations is solved by the Newton-Raphson method with comprehensive initial guesses. The method was applied to a simulated spectrum of CH_2Cl_2 showing good agreement with the data used to simulate the spectrum, which indicates that the approximations used in the method are reasonable. Good results were obtained for the experimental cluster at the molecular ion region of CH_2Cl_2 where the ions M^+, $M\text{-}H^+$, and $M\text{-}2H^+$ were found to be in the approximate ratios of 140:8:1. For the cluster at the region of the $C_7H_{12}^{\cdot+}$ ion from decahydronaphthalene, 6 different formula ions were found ($C_7H_7^+$ to $C_7H_{12}^+$) with the approximate ratios of 1:0:27:10:393:517. The M-nH method was also applied to the elimination of interference from metal hydrides at the mercury cluster of the dimethylmercury electron impact spectrum from the NIST/EPA/NIH database and electrospray mass spectrum of a lead solution from the literature. In this last case, the hydride had a significant amount of deuterium due to the deuterated methanol used as solvent, but, since there were no $M + 2H^+$ and over, a similar mathematical formulation could be used, and the M-nH method was successfully applied. The approximate ratios of Pb^+, Pb^1H^+, and Pb^2H^+ were found to be 60:3:2. (Int J Mass Spectrom 178 (1998) 129–141) © 1998 Elsevier Science B.V.

Keywords: Isotope pattern; Isobaric interference; Low-resolution mass spectrometry; Chemometrics; M-nH ions

---

1. Introduction

Knowledge of isotope patterns of elements, molecules, or ions is useful in many ways. For example, the determination of $^{13}C/^{12}C$ ratios can be used to infer the origin of organic substances for biogeochemistry, archaeology, and adulteration detection in foods and drinks. Stable isotopes can be used in medicine and biochemistry as isotope tracers to diagnose some diseases or to provide information about metabolic routes [1]. By comparing experimental isotope patterns to calculated ones, it is possible to determine the elemental compositions of substances. Some pro-

---

* Corresponding author. E-mail: claudemi@iq.usp.br

[1] Present address: Departamento de Química-ICEx, Universidade Federal de Minas Gerais, Av. Antônio Carlos 6627, CEP 31270-901, Belo Horizonte-MG, Brazil.

PII S1387-3806(98)14081-2

grams have been developed to perform such calculations [2–5].

Mass spectrometry is the most direct technique available to perform such determinations. However, sometimes, there is more than one ion whose mass to charge ratios (*m/z*) are in the region of interest, which results in the appearance of peak clusters that are combinations of their isotope patterns. This interference rarely causes serious troubles in high-resolution mass spectrometers, due to the mass defect. The exact *m/z* values of different ions with the same nominal mass are seldom so close that a high-resolution instrument cannot distinguish them.

On the other hand, if low-resolution mass spectrometers are used, the abundances of the peaks of different ions with the same nominal mass in the cluster are summed up, resulting in single peaks. This superposition makes the determination of the isotope patterns difficult or even impossible. Chemometric procedures to solve these problems are interesting because low-resolution mass spectrometers are less expensive and more common than high-resolution ones and the low-resolution mode has a much higher sensitivity than the high-resolution mode (except for Fourier transform–ion cyclotron resonance mass spectrometers).

The most common kind of isobaric interference in clusters from low-resolution mass spectra of organic compounds is due to ions which differ from the parent ion (M^+) by the loss of one or more hydrogen atoms (M-nH ions). We carried out a statistical study about the frequency of appearance of M-nH ions with 30 spectra of organic compounds with molar masses between 30 and 300 g mol^{-1}, randomly chosen from the literature [6]. The 30 spectra were broken down into 216 clusters, in which those peaks below 5% of the base peak were disregarded. Since only substances composed by C, H, N, O, S, F, Si, P, and few Cl and Br atoms were considered, the M-nH ions were easily detected. M-nH ions with loss of at least one hydrogen were observed in 121 clusters (56%) from 29 spectra (97%). If a smaller threshold value had been used, an even larger number of M-nH occurrences would have been found.

This screening shows that the occurrence of M-nH interference is not the exception, but the rule. However, only two programs for determining elemental compositions from low-resolution mass spectra considering these interferences have been found [4,5]. Nevertheless, they can only treat $M\text{-}1H^+$ ions.

This kind of interference is not restricted to organic mass spectrometry. Determining isotopic ratios of some transition metals by electrospray mass spectrometry, Ketterer and Guzowski noticed the appearance of significant PbH^+ amounts, which made inaccurate the Pb isotopic ratios determination [7]. This is an occurrence of $M{+}nH^+$ ions, which is similar to the former case.

In this paper, we introduce a chemometric procedure to obtain the pure isotope pattern of an element or molecule from the corresponding peak cluster of a low-resolution mass spectrum with M-nH interference.

2. M-nH method

Table 1 shows how a cluster may be understood. In this case, there are three different kinds of ions (M^+, $M\text{-}H^+$, and $M\text{-}2H^+$) in different amounts. In this table and in the following discussion, the part of the elemental composition of the ion that is not involved in the fragmentation process is represented by A, e.g. the cluster present in the spectrum of dichloromethane that comprises CCl^+, $CHCl^{\cdot+}$, and CH_2Cl^+ is understood as composed of A, AH, and AH_2, respectively.

In Table 1, *m* is the lowest m/z of the cluster and c_i is the expected intensity of the peak at m/z equal to $m + i - 1$. Each peak intensity c_i is the sum of the isobaric contributions from the three kinds of ions. The value y_m stands for the amount of the AH_{m-1} ion. The abundance of the ^1H isotope is h_1 and of the deuterium is h_2. The abundance of the ith isotope of the composition A is represented by b_i. Since the isotope patterns are normalized to sum equal to one, therefore being dimensionless, the values of y_m have the same units as the experimental intensities.

Although it is possible to go on with a strict approach, one may disregard the deuterium abun-

Table 1
Scheme for the composition of a cluster[a]

m/z	A		A^1H		A^2H		A^1H_2		A^1H^2H and A^2H^1H		A^2H_2		*Intensity*
m	y_1b_1											$=$	c_1
$m + 1$	y_1b_2	$+$	$y_2h_1b_1$									$=$	c_2
$m + 2$	y_1b_3	$+$	$y_2h_1b_2$	$+$	$y_2h_2b_1$	$+$	$y_3h_1^2b_1$					$=$	c_3
$m + 3$			$y_2h_1b_3$	$+$	$y_2h_2b_2$	$+$	$y_3h_1^2b_2$	$+$	$2y_3h_1h_2b_1$			$=$	c_4
$m + 4$					$y_2h_2b_3$	$+$	$y_3h_1^2b_3$	$+$	$2y_3h_1h_2b_2$	$+$	$y_3h_2^2b_1$	$=$	c_5
$m + 5$									$2y_3h_1h_2b_3$	$+$	$y_3h_2^2b_2$	$=$	c_6
$m + 6$											$y_3h_2^2b_3$	$=$	c_7

[a] The values b_i and h_i are the abundances of the isotope i of the composition A and of the hydrogen, respectively, and y_i is the amount of the ion AH_{i-1}^+ (see text).

dance in order to simplify the calculation. Thus, the contributions of the A^2H, A^1H^2H, and A^2H_2 ions are ignored. Table 2 shows the simplified form of Table 1 for this case. It should be noted that the deuterium contribution to the isotope pattern of the ion A is not disregarded in this approach. In fact, for a large number of hydrogen atoms, the deuterium contribution is important because the probability of ions with this isotope increases. For example, for an ion $C_{100}H_{200}^+$, the expected ratio of the peaks at m/z 1400 and 1401 is 0.869 and if the deuterium is disregarded, the expected ratio becomes 0.891. The greater the number of hydrogen atoms, the greater this discrepancy. However, for the few hydrogen atoms involved in the fragmentation, this approximation is not so imprecise, so that one can consider that the isotope patterns of the M-nH ions have the same abundances, but shifted by one of more mass units. Figure 1 shows graphically this idea that the resulting cluster is the weighted sum of these shifted isotope patterns.

Table 2
Simplified scheme for the composition of a cluster[a]

m/z	A		AH		AH_2		Intensity
m	y_1b_1					$=$	c_1
$m + 1$	y_1b_2	$+$	y_2b_1			$=$	c_2
$m + 2$	y_1b_3	$+$	y_2b_2	$+$	y_3b_1	$=$	c_3
$m + 3$			y_2b_3	$+$	y_3b_2	$=$	c_4
$m + 4$					y_3b_3	$=$	c_5

[a] Assuming insignificant deuterium abundance.

By generalizing Table 2 for a set of p isotopes of A and g different elemental formula ions in the cluster (e.g. g is 3 if there are the ions A^+, AH^+, and AH_2^+), the following equation is obtained:

$$c_j = \sum_{i=\max(1,j-p+1)}^{\min(j,g)} b_{j-i+1} \cdot y_i \tag{1}$$

where the functions min and max are the minimum and maximum values, respectively, of their arguments. The detailed demonstration of Eq. (1) is in Appendix.

The values c_i, b_i, and y_i can be understood as the coordinates of the vectors **c**, **b**, and **y**, respectively. Taking into account that the vectors **b** and **y** are unknown, there are $p + g$ variables that must be mathematically obtained by solving a set of $p + g$ equations. Considering a cluster with n peaks, it can be easily verified (see Appendix) that

$$p + g = n + 1 \tag{2}$$

There are n functions giving zero when the correct values of **y** and **b** are used:

$$f_i(\mathbf{y},\mathbf{b}) = c_i - r_i \tag{3}$$

where i is in the range from 1 to n and **r** represents the experimental peak intensities of the cluster. The last

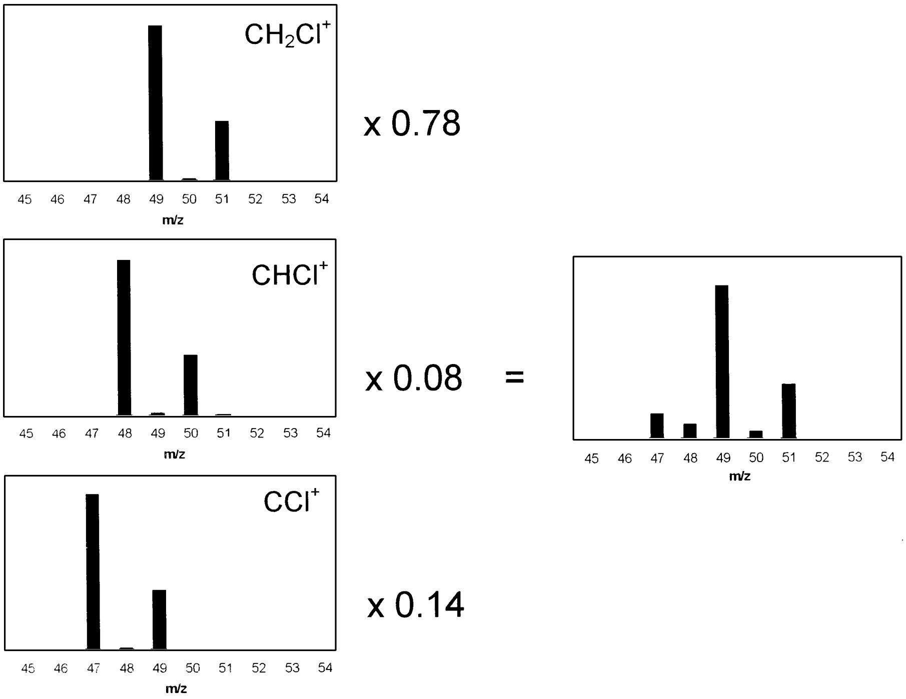

Fig. 1. The cluster on the right side, which is observed in the mass spectrum of dichloromethane, can be understood as the weighted sum of the isotope patterns of CH_2Cl^+, $CHCl^{\cdot+}$, and CCl^+. By disregarding the deuterium contribution, the three patterns on the left side have the same abundances, but shifted on the m/z axis.

function is obtained from another constraint: the isotope pattern **(b)** is normalized to one. Therefore, the function

$$f_{n+1}(\mathbf{b}) = \left(\sum_{i=1}^{p} b_i\right) - 1 \tag{4}$$

is zero for the correct value of **b.**

Due to the nonlinearity of these equations, the Newton-Raphson is a good method to find their roots [8]. This is a well-known iterative algorithm that works through the following recurrence formula for a system of equations:

$$\mathbf{x}_{i+1} = \mathbf{x}_i - \mathbf{J}_i^{-1} \cdot \mathbf{f}_i \tag{5}$$

or, in a more convenient form for numerical methods,

$$\mathbf{J}_i \cdot \Delta = -\mathbf{f}_i \tag{6}$$

where $\mathbf{x}_i$ and $\mathbf{x}_{i+1}$ are current and new values of the vector of variables, respectively, $\mathbf{f}_i$ is the functions vector, $\mathbf{J}_i$ its Jacobian matrix, and Δ is an increment vector $(\mathbf{x}_{i+1} - \mathbf{x}_i)$.

Since the vector of variables is defined as

$$\mathbf{x} = [y_1, y_2, \ldots, y_g, b_1, b_2, \ldots, b_p] \tag{7}$$

and the functions vector as

$$\mathbf{f} = [f_1, f_2, \ldots, f_n, f_{n+1}] \tag{8}$$

the Jacobian matrix for a case of $p = 2$ and $g = 3$ is given by

$$\mathbf{J} = \begin{bmatrix} b_1 & 0 & 0 & y_1 & 0 \\ b_2 & b_1 & 0 & y_2 & y_1 \\ 0 & b_2 & b_1 & y_3 & y_2 \\ 0 & 0 & b_2 & 0 & y_3 \\ 1 & 1 & 1 & 1 & 1 \end{bmatrix} \tag{9}$$

The convergence is accomplished when the magnitude of Δ is small enough. The criterion of convergence may be obtained in numerical or statistical

Table 3
Natural isotopic abundances and the simulated cluster for the molecular ion region of CH_2Cl_2

Cluster		C		Cl		H		Amounts	
m	Abund.	*m*	Abund.	*m*	Abund.	*m*	Abund.	Ion	Abund.
82	$3.9745586147 \times 10^{-3}$	12	0.9890	35	0.7577	1	0.99985	$CCl_2^{\cdot+}$	0.007
83	3.0700488×10^{-2}	13	0.0110	36	0	2	0.00015	$CHCl_2^{+}$	0.054
84	$5.358862787 \times 10^{-1}$			37	0.2423			$CH_2Cl_2^{\cdot+}$	0.939
85	$2.57231932 \times 10^{-2}$								
86	$3.415176966 \times 10^{-1}$								
87	$7.0332725559 \times 10^{-3}$								
88	$5.45417435 \times 10^{-2}$								
89	$6.2258569495 \times 10^{-4}$								
90	$1.8312192489 \times 10^{-7}$								
91	$1.3644185769 \times 10^{-11}$								

bases. Our implementation uses a numerical criterion (to iterate until $|\Delta|^2 < 10^{-20}$) because it is simple and generic.

Another important point in this procedure is the initial guesses for **b** and **y**. If they are not close enough to the actual values, the method may converge to an undesired solution. Since the program is very quick, the procedure is repeated for some initial guesses to find a set of solutions in a physically meaningful geometrical space.

There are two constraints to this space: (i) vector **b** is normalized to one [Eq. (4)], (ii) there are no peaks with negative intensities, i.e. $b_i \geq 0$. These constraints generate a simplex polytope. The initial guesses to the isotope pattern may be graphically represented as vertexes, centers of edges, faces, and body of the simplex.

Setting all peaks (b_i) to $1/p$, the guess is the center of the simplex. Setting one peak to zero and the others to $1/(p - 1)$, a frontier of the simplex is reached. For two peaks set to zero, other frontiers are obtained, and so on. The last frontiers are the vertexes, i.e. all peaks but one are zero. The number of possibilities is $2^p - 1$.

The guess for **y** is obtained by multiple linear regression to find the best fit of the proposed **b** and the vector of experimental peaks, **r**.

Because analytical functions that relate **b** and **y** to **r** are unknown, it is not possible to obtain straightforwardly standard deviation estimates for the elements of vectors **b** and **y**. Thus, we decided to use the following numerical approach.

A set of results is obtained by applying the M-nH method to **r** vectors modified by changing one of the experimental intensities each time. Two values are used for each peak: its abundance minus and plus its standard deviation, respectively. The set of **b** and **y** vectors thus obtained is used to calculate numerical approximations to the partial derivatives of the M-nH method results with respect to the experimental intensities. The variances of the results are then estimated through the usual formula:

$$\sigma(b \text{ or } y)_i^2 = \sum_{j=1}^{n} \left(\frac{\partial (b \text{ or } y)_i}{\partial r_j} \right)^2 \sigma r_j^2 \tag{10}$$

3. Experimental

3.1. Implementation

Formerly, the M-nH method was designed to be a tool for programs that determine elemental compositions through isotope patterns. Thus, it was implemented as a Turbo Pascal (Borland) unit. However, it is not restricted to such kind of programs and a generic one that works with any cluster, inputted as an ASCII file, was developed using Borland Delphi 2.0.

3.2. Apparatus

Spectra were obtained with electron energy scanning in a pentaquadrupole mass spectrometer inter-

Table 4
M-nH result for the molecular ion cluster of CH_2Cl_2

Isotope pattern				Amounts	
m/z[a]	Obtained abundance	Expected abundance for the $CCl_2^{\cdot+}$	Expected abundance for the $CH_2Cl_2^{\cdot+}$	Ion	Abundance
	$5.676301956 \times 10^{-1}$	$5.677940878 \times 10^{-1}$	$5.676237624 \times 10^{-1}$	$CCl_2^{\cdot+}$	$7.002021114 \times 10^{-3}$
$m + 1$	$6.473009590 \times 10^{-3}$	$6.315202190 \times 10^{-3}$	$6.483620447 \times 10^{-3}$	$CHCl_2^{+}$	$5.400551995 \times 10^{-2}$
$m + 2$	$3.630391175 \times 10^{-1}$	$3.631424244 \times 10^{-1}$	$3.630353969 \times 10^{-1}$	$CH_2Cl_2^{\cdot+}$	$9.389822758 \times 10^{-1}$
$m + 3$	$4.146748861 \times 10^{-3}$	$4.038995620 \times 10^{-3}$	$4.146710540 \times 10^{-3}$		
$m + 4$	$5.804788537 \times 10^{-2}$	$5.806348780 \times 10^{-2}$	$5.804728980 \times 10^{-2}$		
$m + 5$	$6.630430744 \times 10^{-4}$	$6.458021900 \times 10^{-4}$	$6.630249882 \times 10^{-4}$		
$m + 6$			$1.950180243 \times 10^{-7}$		
$m + 7$			$1.453054928 \times 10^{-11}$		

[a] $m = 82$ and 84 u for $CCl_2^{\cdot+}$ and $CH_2Cl_2^{\cdot+}$, respectively.

faced to a 486 DX 50-MHz microcomputer [9]. This equipment was used because we had access to the source code of the data acquisition software, so that the electron energy scanning could be easily implemented. Commercially available instruments do not have this tool and seldom their manufacturers provide the necessary information for its implementation.

The samples were introduced with an unheated direct insertion probe. The electron energy was varied in the range from 5.0 to 70.0 eV, with increments from 0.1 to 2.0 eV. The spectra were obtained at the region from m/z 12 u to a little above the heaviest peak of the molecular ion of each used compound.

3.3. Materials and reagents

Samples of dichloromethane and decahydronaphthalene were used without previous purification.

4. Results and discussion

In order to demonstrate the applicability of the method, some clusters of some spectra were selected. However, before the application to experimental data, the results for ideal spectra will be shown. Such ideal spectra should be understood as those obtained in an hypothetical instrument without instrumental mass discrimination, isotopic fractionation, and with good signal-to-noise ratio. These spectra were generated by simulation, considering the amounts of M-nH ions similar to those obtained in experimental spectra.

The method was applied to a simulated cluster at the region of the molecular ion of dichloromethane. The ions considered were $CH_2Cl_2^{\cdot+}$, $CHCl_2^{+}$, and $CCl_2^{\cdot+}$. The spectrum was simulated by linearly combining the isotope patterns of these three ions, calculated by polynomial expansion from the natural iso-

Table 5
M-nH result considering standard deviations for the molecular ion cluster of CH_2Cl_2

Isotope pattern		Amounts	
m/z[a]	Abund.	Ion	Abund.
m	$(5.676302 \pm 0.000007) \times 10^{-1}$	$CCl_2^{\cdot+}$	$(7.0020 \pm 0.0008) \times 10^{-3}$
$m + 1$	$(6.4730 \pm 0.0006) \times 10^{-3}$	$CHCl_2^{+}$	$(5.40056 \pm 0.00008) \times 10^{-2}$
$m + 2$	$(3.630391 \pm 0.000006) \times 10^{-1}$	$CH_2Cl_2^{\cdot+}$	$(9.38982 \pm 0.00001) \times 10^{-1}$
$m + 3$	$(4.1468 \pm 0.0005) \times 10^{-3}$		
$m + 4$	$(5.80478 \pm 0.00005) \times 10^{-2}$		
$m + 5$	$(6.630 \pm 0.005) \times 10^{-4}$		

[a] $m = 82$, 83, and 84 u for $CCl_2^{\cdot+}$, $CHCl_2^{+}$, and $CH_2Cl_2^{\cdot+}$, respectively.

Table 6
Experimental cluster of dicloromethane spectrum[a]

m/z	Intensity (A.U.)[b]
82	$(2.0 \pm 0.7) \times 10^2$
83	$(1.4 \pm 0.1) \times 10^3$
84	$(2.38 \pm 0.01) \times 10^4$
85	$(1.23 \pm 0.08) \times 10^3$
86	$(1.529 \pm 0.003) \times 10^4$
87	$(2.6 \pm 0.4) \times 10^2$
88	$(2.28 \pm 0.06) \times 10^3$

[a] Spectrum at 50-eV electron energy
[b] A.U. stands for arbitrary units.

tope patterns of C, H, and Cl. The deuterium abundance was not disregarded in calculating the cluster. Table 3 shows the simulated cluster, as well as the natural isotope patterns of C, H, and Cl and the amounts of the M-nH ions.

Because the isotope pattern of $CCl_2^{\cdot+}$ has only six peaks and it is assumed to be equal to that of the other two ions (deuterium abundance is disregarded in the fragmentation), the last two peaks of the simulated cluster ($m/z = 90$ and 91) were disregarded so that $p = 6$, $g = 3$, and $n = 8$. Table 4 shows the results of the method, as well as the expected isotope pattern of the $CCl_2^{\cdot+}$ and $CH_2Cl_2^{\cdot+}$ for comparison purposes. The results match very closely the two isotope patterns, but there are some small discrepancies, which are due to the approximation of zero deuterium abundance done in the M-nH method. One can notice that the results match the $CH_2Cl_2^{\cdot+}$ isotope pattern closer than that of $CCl_2^{\cdot+}$. This is a feature of the method: Its results are always closer to the isotope pattern of the most abundant ion ($CH_2Cl_2^{\cdot+}$ in this case) than to those of the others. At any rate, these differences are small when compared to the usual magnitudes of experimental errors.

To illustrate the scheme of error propagation in the method, the previous calculation was repeated considering that the standard deviations of the intensities of the peaks in the simulated cluster were equal to 0.000 000 5 (1 millionth of the intensity of the base peak). Table 5 shows that the magnitudes of the calculated standard deviations are compatible with those of the simulated cluster.

More than one solution was obtained in the above applications of the method, as expected. Because the isotope pattern was known, the correct solution was selected by ourselves. For actual cases, other considerations will be discussed, as follows. The next results were obtained using experimental data from actual spectrometers. Because the conditions were not ideal, these examples are more daring challenges to the method.

4.1. Dichloromethane

Spectra of a dichloromethane sample were obtained with electron energies between 8 and 50 eV and 1-eV increments. The inspection of the cluster from 82 to 88 u indicates the presence of three ions, corresponding to $CH_2Cl_2^{\cdot+}$, $CHCl_2^+$, and $CCl_2^{\cdot+}$.

The M-nH method was applied to the spectrum obtained at 50 eV (Table 6), which has the best signal-to-noise ratio, and all the 31 possible initial guesses were tried. Results containing negative numbers with absolute values greater than three times their

Table 7
M-nH results for dichloromethane[a]

Result 1[b]		Result 2		Result 3	
Isotope pattern	Amounts	Isotope pattern	Amounts	Isotope pattern	Amounts
0.568 ± 0.002	$CCl_2^{\cdot+}$ $(3 \pm 1) \times 10^2$	0.005 ± 0.002	$(3.57 \pm 0.04) \times 10^4$	0.006 ± 0.002	$(3.15 \pm 0.05) \times 10^4$
0.008 ± 0.002	$CHCl_2^+$ $(2.4 \pm 0.2) \times 10^3$	0.039 ± 0.003	$(4 \pm 4) \times 10^2$	0.044 ± 0.003	$(1 \pm 4) \times 10^2$
0.366 ± 0.002	$CH_2Cl_2^{\cdot+}$ $(4.17 \pm 0.02) \times 10^4$	0.666 ± 0.009	$(8.4 \pm 0.4) \times 10^3$	0.75 ± 0.01	$(1.29 \pm 0.04) \times 10^3$
0.0031 ± 0.0009		0.018 ± 0.008		0.019 ± 0.008	
0.055 ± 0.001		0.272 ± 0.008		0.176 ± 0.009	

[a] Spectrum at 50 eV from the same experiment shown in Table 3.
[b] The isotope pattern indicates that this is the correct result.

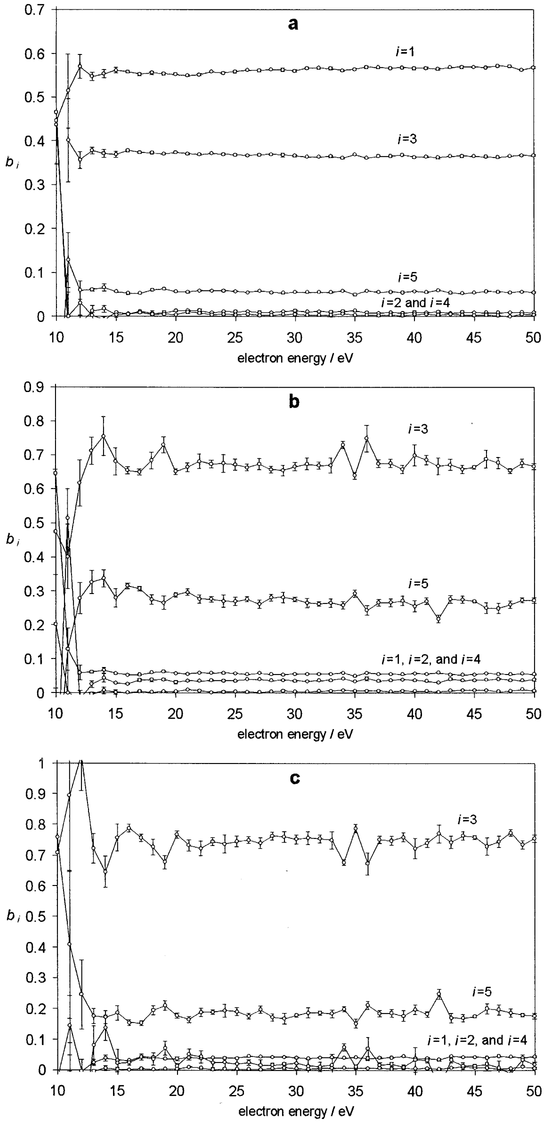

Fig. 2. Vector **b** vs electron energy for the dichloromethane cluster from 82 to 88 u. Plots a, b, and c were obtained with solutions 1, 2, and 3, respectively; see Table 7.

own standard deviations were discarded. This was done because, in these cases, the null hypothesis could be rejected at 99.7% probability level and there is no sense in negative abundances. Three results were left, which are shown in Table 7.

Depending on the case being treated, other considerations can also be done. Presuming that one knows that the spectrum is from an organic substance with none or a small number of N, O, F, Cl, Br, S, Si, and P atoms, results 2 and 3 can be discarded, because the lightest isotopes from the patterns are scarce. Thus, the only remaining result is the first one, which is the correct solution. On the other hand, if boron is present in the molecule, this consideration cannot be easily done.

Figure 2 shows plots of vector **b** against the electron energy for the three possible solutions. The data for solution 1 [Fig. 2(a)] have a much smaller variance than that for solutions 2 and 3 [Figs. 2(b) and (c), respectively]. As the vector **b** is expected not to vary with the electron energy scanning, one can conclude from the plots that solution 1 is the correct one.

Direct examination of the 50-eV cluster of dichloromethane at the region from 47 to 52 u (Table 8) indicates the presence of three components, corresponding to CH_2Cl^+, $CHCl^{\cdot+}$, and CCl^+. The M-nH method was applied to this cluster and all the 15 initial guesses were tried. Only two acceptable results were obtained, which are shown in Table 9. Result 1 matches the isotope pattern of the dichloromethane fragments, while result 2 cannot be explained based on combinations of the just cited elements.

Figure 3 contains plots of vector **b** as a function of the electron energy for the solutions 1 and 2. Fig. 3(b) presents a clear tendency of **b** to vary over a wide range of electron energies (about 15 to 35 eV). On the other hand, vector **b** in Fig. 3(a) tends to remain constant along the whole range of electron energies,

Table 8
Experimental cluster of dicloromethane spectrum[a]

m/*z*	Intensity (A.U.)[b]
47	(1,010 ± 0.008) × 10^4
48	(6,08 ± 0.006) × 10^3
49	(6,01 ± 0.02) × 10^4
50	(2,92 ± 0.08) × 10^3
51	(2,149 ± 0.006) × 10^4
52	(1,7 ± 0.5) × 10^2

[a] Spectrum at 50 eV electron energy
[b] A.U. stands for arbitrary units.

Table 9
M-nH results for dichloromethane[a]

Result 1[b]		Result 2	
Isotope pattern	Amounts	Isotope pattern	Amounts
0.716 ± 0.001	CCl^+ (1.41 ± 0.01) × 10^4	0.139 ± 0.001	(7.28 ± 0.03) × 10^4
0.008 ± 0.001	$CHCl^{\cdot+}$ (8.34 ± 0.09) × 10^3	0.0831 ± 0.0009	(2 ± 2) × 10^2
0.274 ± 0.001	CH_2Cl^+ (7.84 ± 0.02) × 10^4	0.772 ± 0.002	(2.78 ± 0.01) × 10^4
0.0022 ± 0.0006		0.006 ± 0.002	

[a] Spectrum at 50 eV from the same experiment shown in Table 5.
[b] The isotope pattern indicates that this is the correct result.

except for the very beginning. Again, as **b** is expected not to vary with the electron energy, one can conclude from the curves that solution 1 is the correct one.

The low electron energy region of Fig. 3(a) shows a $^{35}Cl/^{37}Cl$ ratio above the naturally expected. The isotopic ratio tends to decrease and get stabilized near its natural value as the energy is increased. This may be explained by improper base line or isotopic fractionation—because the C–^{35}Cl bond is more easily broken than the C^{37}Cl—which are more pronounced at low electron energies.

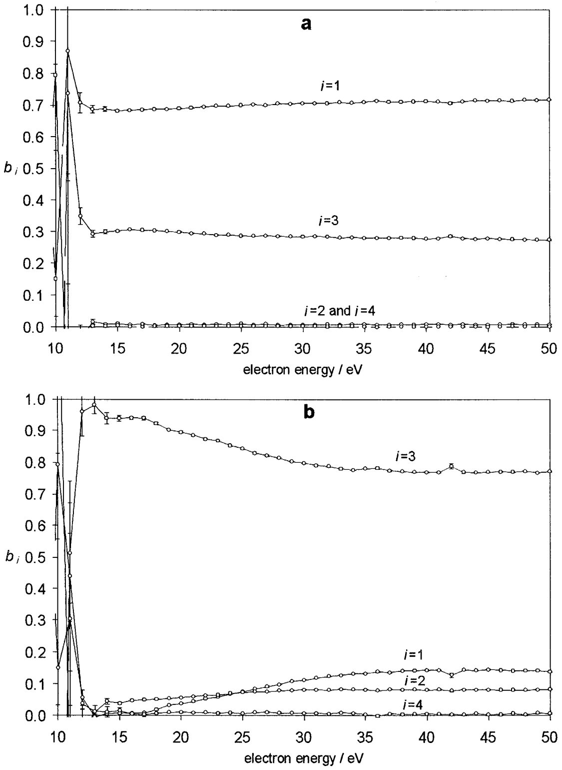

Fig. 3. Vector **b** vs electron energy for the dichloromethane cluster from 47 to 52 u. Plots a and b were obtained with solutions 1 and 2, respectively; see Table 9.

The analysis of Figs. 2 and 3 shows an interesting feature: sometimes, it is possible to exclude the solutions whose **b** versus *E* curves show large variations.

4.2. Decahydronaphthalene

For the cluster from m/z 91 to 97 of the decahydronaphthalene spectrum (Table 10), $g = 6$ and $p = 2$ were used. Again, from the 3 initial guesses, only one admissible result, which is compatible with the C_7H_{12} isotope pattern, was achieved (Table 11). It should be noted that, although M-4H$^+$ has a negative amount, from a statistical point of view, it is only possible to say that this ion does not have a significant amount.

This last example (decahydronaphthalene) is oppo-

Table 10
Experimental cluster of decahydronaphthlene spectrum[a]

m/z	Intensity (A.U.)[b]
91	(8.5 ± 0.7) × 10^2
92	(4 ± 6) × 10
93	(2.2 ± 0.1) × 10^3
94	(9.9 ± 0.8) × 10^2
95	(3.27 ± 0.02) × 10^4
96	(4.56 ± 0.04) × 10^4
97	(3.66 ± 0.06) × 10^3

[a] Spectrum at 30 eV electron energy.
[b] A.U. stands for arbitrary units.

Table 11
M-nH results for decahydronaphthalene[a]

Isotope pattern	Amounts
0.921 ± 0.001	$C_7H_7^+$ (9 ± 7) × 10
0.079 ± 0.001	$C_7H_8^{\cdot+}$ (−4 ± 6) × 10
	$C_7H_9^+$ (2.4 ± 0.1) × 10^3
	$C_7H_{10}^{\cdot+}$ (8.7 ± 0.8) × 10^2
	$C_7H_{11}^+$ (3.54 ± 0.03) × 10^4
	$C_7H_{12}^{\cdot+}$ (4.65 ± 0.04) × 10^4

[a] Spectrum at 30 eV from the same experiment shown in Table 7.

site to the previous cases, where a few number of ions with complex isotope patterns were present.

4.3. Mercury

As already mentioned in the introduction, the M-nH method can be applied to systems with gain instead of loss of hydrogen atoms (formation of M + nH^+ ions). One such case is the determination of mercury isotope pattern from the spectrum of $Hg(CH_3)_2$ with electron impact ionization.

Table 12 contains the cluster from 196 to 205 u of the NIST/EPA/NIH library spectrum of $Hg(CH_3)_2$, corresponding to Hg^+. Because ^{203}Hg is radioactive and there is no 205 isotope of mercury (see Table 13) one can deduce the presence of a M + $1H^+$ ion (HgH^+) because the peaks at *m/z* 203 and 205 u have significant intensities. The M-nH method was applied to this 10-peak cluster considering standard deviations to be equal to 0.1, $p = 9$, and $g = 2$. From the 511 initial guesses, only 3 solutions were obtained, which are in Table 13. Solution 1 contains the expected isotope pattern of Hg, in good agreement with the natural abundances.

In a recent article, Hintelmann et al. describe the use of a GC/ICP-MS to measure mercury methylation through enriched stable isotopes [10]. The ICP destroys the organometallic compounds, releasing Hg without contamination. Thus, M-nH may also be employed as an alternative method, making possible the use of a conventional GC/MS with electron impact ion source. Of course, another advantage of the use of ICP is the decomposition of almost all compounds, so that most other common organic substances with close chromatographic retention time will not interfere at the region of *m/z* 200. Even so, this is a separation rather than spectrometric task.

Table 12
Spectrum of $Hg(CH_3)_2$[a]

m/z	Intensity (A.U.)[b]
196	0.20
197	0.20
198	12.40
199	22.80
200	31.20
201	19.60
202	39.20
203	4.00
204	8.40
205	0.80

[a] Data from the NIST/EPA/NIH library.
[b] A.U. stands for arbitrary units.

Table 13
M-nH results for Hg[a]

Isotope pattern		
Calculated	Natural[b]	Amounts
0.0016 ± 0.0008	0.0015	Hg^+ (1.27 ± 0.01) × 10^2
0.0014 ± 0.0008	—	HgH^+ (1.2 ± 0.1) × 10
0.098 ± 0.001	0.1002	
0.171 ± 0.001	0.1684	
0.2300 ± 0.0009	0.2313	
0.133 ± 0.001	0.1322	
0.297 ± 0.002	0.298	
0.003 ± 0.003	Radioactive	
0.066 ± 0.001	0.0685	

[a] Cluster from *m/z* 196 to 205 *u* from the NIST/EPA/NIH library spectrum.
[b] Literature data [10].

Table 14
Experimental cluster of lead[a]

m/z	Intensity (mm)
204	1.0 ± 0.5
205	0.5 ± 0.5
206	12.0 ± 0.5
207	11.0 ± 0.5
208	37.0 ± 0.5
209	2.0 ± 0.5
210	1.0 ± 0.5

[a] Spectrum obtained from literature data [7]; see text.

Table 15
Simplified scheme for the composition of a cluster[a]

m/z	A		A^1H		A^2H		Intensity
m	y_1b_1					=	c_1
$m + 1$	y_1b_2	+	$y_2h_1b_1$			=	c_2
$m + 2$	y_1b_3	+	$y_2h_1b_2$	+	$y_2h_2b_1$	=	c_3
$m + 3$			$y_2h_1b_3$	+	$y_2h_2b_2$	=	c_4
$m + 4$					$y_2h_2b_3$	=	c_5

[a] Assuming the unique presence of M-1H ions.

4.4. Lead

Another case of hydride interference occurs in the determination of Pb isotope ratios by electrospray mass spectrometry [7]. In this experiment, there is formation of PbH^+, whose isotope pattern superposes that of Pb^+, making its accurate determination very difficult.

Peak heights were directly measured from Fig. 3, in the original paper, with a ruler and are shown in Table 14. Their standard deviations were assumed to be equal to 0.5 mm. Since the spectrum was obtained in deuterated methanol, significant amounts of Pb^2H were formed along with Pb^1H^+. Even so, the M-nH method can be applied to obtain the Pb isotope pattern. This is possible because: (i) there is no $M + 2H^+$ or above and (ii) the deuterium has a significant abundance. Table 15 is a simplified form of Table 1 with these two constraints. By comparing it with Table 2, one can note that, although the physical situation is different, the mathematical formulation is the same from the point of view of the vector **b.** The only difference is that vector **y** is $[y_1, y_2h_1, y_2h_2]$ in Table 15, instead of $[y_1, y_2, y_3]$. In this case, vector **y** is not the vector of amounts of different elemental formula ions. It is worth recalling that the method cannot treat the simultaneous presence of generic M-nH ions and high deuterium content (Table 1).

The M-nH method was applied to the 7-peak cluster of Table 14 considering $p = 5$ and $g = 3$. The 31 initial guesses were tried and only three acceptable results were obtained, which are in Table 16. Solution 1 contains the expected isotope pattern of Pb.

According to the authors, changes in the ion source design to reduce PbH^+ yields are being investigated. The M-nH method could be used to complement experimental improvements.

It should be noted that the M-nH method does not work correctly, unless all the ions composing the cluster are M-nH. This may happen with some aldehydes and ketones because some intermediary fragments can loose CO or C_2H_x to form ions with different isotope patterns, but near *m/z*.

As already mentioned, programs for the determination of elemental compositions need clean isotope patterns to perform their calculations. The fact that the occurrence of M-nH interference is so common may account for the low acceptance of these programs. The M-nH method is a practical solution to these problems. For example, Fig. 4 shows the experimental cluster of $C_7H_{12}^{\cdot+}$ ion and other fragments from decahydronaphthalene, the result of the method and the expected pattern. It seems clear that a better result would be obtained by comparing the expected isotope pattern with the result of the method than with the experimental cluster. The same applies to the CH_2Cl^+ and M-nH fragments from dichloromethane.

Table 16
M-nH results for Pb

Result 1[a]		Result 2		Result 3	
Isotope pattern	Amounts	Isotope pattern	Amounts	Isotope pattern	Amounts
0.017 ± 0.008	Pb^+ (6.0 ± 0.1) × 10	0.15 ± 0.02	7 ± 4	0.10 ± 0.05	(1.0 ± 0.1) × 10
0.008 ± 0.008	Pb^1H^+ 2.8 ± 0.8	0.23 ± 0.05	−7 ± 8	−0.1 ± 0.1	(1.5 ± 0.3) × 10
0.199 ± 0.008	Pb^2H^+ 1.7 ± 0.8	0.57 ± 0.04	(6.5 ± 0.5) × 10	0.93 ± 0.07	(3.9 ± 0.3) × 10
0.174 ± 0.008		0.033 ± 0.008		0.04 ± 0.01	
0.60 ± 0.01		0.015 ± 0.008		0.03 ± 0.01	

[a] The isotope pattern indicates that this is the correct result.

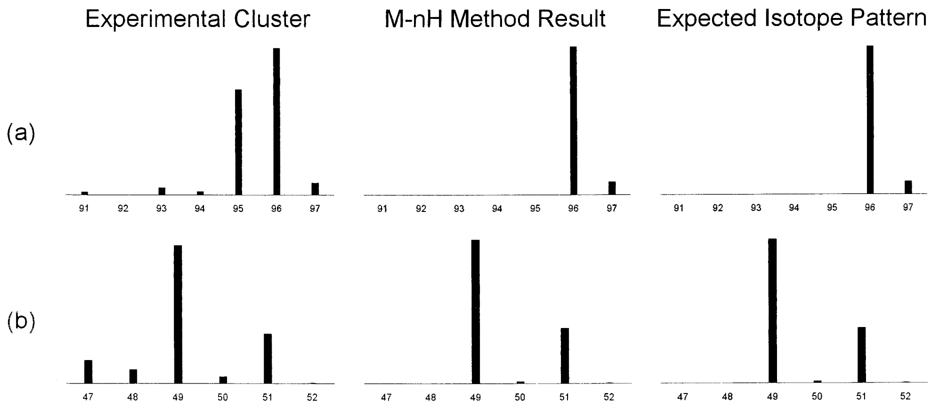

Fig. 4. Mass spectra of the (A) $C_7H_{12}^{\cdot+}$ and (B) CH_2Cl^+ from, respectively, decahydronaphthalene and dichloromethane, the M-nH method results, and expected isotope patterns.

Acknowledgements

This work was supported by the Conselho Nacional de Desenvolvimento Científico e Tecnológico (CNPq) and Fundação de Amparo à Pesquisa do Estado de São Paulo (FAPESP). The authors thank CNPq for the research fellowships, Professor Dr. M. N. Eberlin (Instituto de Química—Unicamp) for the use of the pentaquadrupole mass spectrometer, and E.M. Richter for the English revision.

Appendix

Eq. (1) is obtained by the following considerations. Let g and p be the number of different elemental formula ions (A, AH, . . . , AH_{g-1}) and the number of peaks in the isotope pattern of the A ion, respectively. Let m_0 be the mass of the lightest isotope of the A ion. The lowest and the highest mass in the experimental cluster will be

$$m_{\min} = m_0 \tag{11}$$

$$\begin{aligned} m_{\max} &= m_0 + (g-1) + (p-1) \\ &= m_0 + p + g - 2 \end{aligned} \tag{12}$$

The number of peaks in the cluster will be

$$n = m_{\max} - m_{\min} + 1 = p + g - 1 \tag{13}$$

Also, the mass of the kth isotope of the ion AH_{i-1} will be

$$m_{k,i} = m_0 + (k-1) + (i-1) = m_0 + k + i - 2 \tag{14}$$

The intensity of the jth peak in the experimental cluster (i.e. the one whose mass is $m_0 + j - 1$) will be given by the isobaric contributions of all ions weighted by their respective abundances:

$$c_j = \sum_{m_{k,i}=m_0+j-1} b_k y_i, \tag{15}$$

for j from 1 to n. By substituting (14) in the condition of the summation (15), ($m_{k,i} = m_0 + j - 1$), it becomes

$$c_j = \sum_{k=j-i+1} b_k y_i = \sum_i b_{j-i+1} y_i \tag{16}$$

The limits of this summation are found by imposing limits on i and $j - i + 1$. Because $i \geq 1$ and $j - i + 1 \leq p$, the lower limit on i is max $(1, j - p + 1)$. On the other hand, because $i \leq g$ and $j - i + 1 \geq 1$, the upper limit is min (j,g). Thus, Eq. (16) becomes

$$c_j = \sum_{i=\max(1,j-p+1)}^{\min(j,g)} b_{j-i+1} y_i \tag{17}$$

which is the same as Eq. (1).

References

[1] W.A. Brand, J. Mass Spectrom. 31 (1996) 225.
[2] K.F. Blom, Org. Mass Spectrom. 23 (1988) 194.
[3] P.E. Kavanagh, Org. Mass Spectrom. 15 (1980) 334.
[4] A. Tenhosaari, Org. Mass Spectrom. 23 (1988) 236.
[5] C.L. Lago, C. Kascheres, Comput. Chem. 15 (1991) 149.
[6] F.W. McLafferty, D.B. Stauffer, The Wiley/NBS Registry of Mass Spectral Data, Wiley, New York, 1989.
[7] M.E. Ketterer, J.P. Guzowski Jr., Anal. Chem. 68 (1996) 883.
[8] W.H. Press, B.P. Flannery, S.A. Teukolsky, W.T. Wetterling, Numerical Recipes: The Art of Scientific Computing, Cambridge University Press, Cambridge, 1993, Chap. 9.
[9] V.F. Juliano, F.C. Gozzo, M.N. Eberlin, C. Kascheres, C.L. Lago, Anal Chem. 68 (1996) 1328.
[10] H. Hintelmann, R.D. Evans, J.Y. Villeneuve, J. Anal. At. Spectrom. 10 (1995) 619.
[11] S. Bauerschmidt, W. Hanebeck, K. Schulz -P, Gasteiger, J. Anal. Chim. Acta. 265 (1992) 169.
[12] B.D. Holt, N.C. Sturchio, T.A. Abrajano, L.J. Heraty, Anal. Chem. 69 (1997) 2727.